International Journal of Thermal Sciences 48 (2009) 1574–1585

Contents lists available at ScienceDirect

International Journal of Thermal Sciences

www.elsevier.com/locate/ijts

Optimum ventilation based on the overall ventilation effectiveness for temperature distribution in ventilated cavities

J. Xamán [a,*], J. Tun [b,1], G. Álvarez [a], Y. Chávez [a], F. Noh [a]

[a] Centro Nacional de Investigación y Desarrollo Tecnológico (CENIDET-DGEST-SEP), Prol. Av. Palmira S/N, Col. Palmira, Cuernavaca, Morelos, CP 62490, Mexico
[b] Instituto Mexicano del Petróleo (Competencia de Producción de Hidrocarburos) (IMP), Av. Periférica Norte ·#75, Esq. Calle 35B, Col. San Agustín del Palmar, Cd. Del Carmen, Campeche, CP 24118, Mexico

ARTICLE INFO

Article history:
Received 2 February 2008
Received in revised form 1 October 2008
Accepted 14 December 2008
Available online 15 January 2009

Keywords:
Conjugated heat transfer
Displacement ventilation

ABSTRACT

A numerical study of conjugated heat transfer in a ventilated cavity was carried out in order to analyze temperature distribution effectiveness inside it, and to determine a good ventilation configuration. The space was represented by a ventilated cavity under turbulent flow regime. All the walls were considered adiabatic, except the vertical wall on right, which was defined as a conductive opaque wall with a gap in its lower side for the incoming air. The conductive wall is submitted to a constant heat flux of 736 W/m^2 and it is considered to interact with the outside ambient. Four cases for the air exhaust location were considered for the analysis; the incoming air velocity was varying depending on the Reynolds number between $2 \times 10^3 \leqslant Re \leqslant 4 \times 10^4$. The conductive wall was analyzed for two different materials (construction brick and adobe block) and three different widths each (0.1, 0.2 and 0.3 m). The mass, momentum and energy equations, coupled with the turbulence model k–ε were discretized in finite volumes. From the results can be concluded that the 0.3 m width adobe block is the appropriate to minimize thermal load gains to the inside of the room and it helps to reduce the efforts made on ventilation to remove heat. Regarding the air exhaust location, it was concluded that the right side of the upper horizontal wall was the best position for the air exhaust for a Reynolds number between 5×10^3 and 1×10^4 based on the effectiveness of temperature distribution and velocity according to ASHRAE Standard 55, Thermal environment conditions for human occupancy, 2004 [1].

1. Introduction

Air is an abundant fluid that can be used in an effective way for cooling or heating in many applications such as cooling of electronic equipment, buildings thermal design, air conditioning equipment, etc. In particular, a good knowledge of air behavior in ventilated rooms is essential for designing ventilation systems; the goal is to create a suitable environment where a good velocity and air temperature as well as contaminants concentration prevail. The process for creating an adequate interior microclimate basically can be divided in two categories: ventilation to obtain air of good quality and heating or cooling to achieve thermal comfort. There exist two ventilation methods to obtain a flow distribution of mixed air: (1) mixing ventilation, where the air is supplied into the ventilated space by a turbulent air jet and (2) displacement ventilation, where the air is supplied at a low velocity [2]. On mixing ventilation, air is supplied by a device located on the upper side of the room to mix supplied air with the room air. On displacement ventilation, cold air is supplied on the lower side of the room to displace hot air out of the room, which is released on the upper side. The information on this paper focuses on displacement ventilation with high inlet velocities in order to obtain thermal comfort inside rooms, where a room is modeled as a rectangular cavity with an air inlet and an air outlet. A literature review on different numerical studies on ventilation was carried out and it is presented next.

Regarding laminar regime Papanicolaou and Jaluria [3–5] carried out investigation about mixed convection in a cavity, with a fix heat source. The authors reported in [3] and [4] that flow patterns describe oscillating patterns due to floating forces generated by the heat source, and cooling efficiency improves if the air outlet is located on the lower side of the vertical wall; later in [5], the authors extended the study to an inclined channel, and they concluded that the best behavior on heat transfer is found on vertical channels. Another configurations and heat flux conditions in ventilated cavities were analyzed by Raji and Hasnaoui [6–9]. On recent works Raji and Hasnaoui evaluated the radiation effect on mixed convection in a cavity with an aspect ratio of 2. Results showed

* Corresponding author. Tel.: +52 (777) 3 62 77 70; fax: +52 (777) 3 62 77 95.
E-mail addresses: jxaman@cenidet.edu.mx (J. Xamán), jmtun@imp.mx (J. Tun), gaby@cenidet.edu.mx (G. Álvarez), ycchena@cenidet.edu.mx (Y. Chávez), felipenoh@hotmail.com (F. Noh).
[1] Tel.: +52 (938) 3 81 20 00.

1290-0729/$ – see front matter
doi:10.1016/j.ijthermalsci.2008.12.008

Nomenclature

Cp	specific heat at constant pressure	J/kg K
$C_{1\varepsilon}, C_{2\varepsilon}, C_{3\varepsilon}, C_{\mu}$	constants of the turbulence model	
g	gravity acceleration	m/s^2
h	heat transfer convective coefficient	W/m^2 K
W_m	width of opaque wall	m
L	height of the gap for the inlet or exhaust air	m
H, W	height and width of the cavity	m
Nu	average Nusselt number	
P	pressure	Pa
Q	heat flux	W/m^2
Re	Reynolds number, $\rho u_{\text{in}} L_{\text{in}}/\mu$	
T	air temperature	°C
T_m	wall temperature	°C
T_{ext}	outside ambient temperature	°C
T_{∞}	reference temperature	°C
u, v	horizontal and vertical components of velocity	m/s
x, y	horizontal and vertical coordinates	

Greek symbols

α	thermal diffusivity	m^2/s
β	volume expansion coefficient	K^{-1}
ε	rate of dissipation of k	m^2/s^3
k	turbulence kinetic energy	m^2/s^2
λ	air thermal conductivity	W/m K
λ_m	thermal conductivity of the wall	W/m K
μ	air dynamic viscosity	kg/m s
ρ	air density	kg/m^3

Subscripts

cond	heat conduction
conv	heat convection
ext	outside of the cavity
m	opaque wall
in	inlet
int	inside of the cavity
out	outlet
rad	heat radiation
ref	reference value

that radiation contributes to the homogenization over temperature distribution and a decrease on the maximum temperature inside the cavity can be observed [9]. Singh and Sharif [10] carried out a study with 6 different configurations of inlet and outlet of air. Their results showed that the best configuration in order to improve cooling efficiency of the cavity was the one with the inlet on the lower side of the cold wall and the outlet on the upper side of the hot wall. More recently, Rahman et al. [11], evaluated the combined effect of the Prandtl (Pr), Reynolds (Re) and Richardson (Ri) numbers over mixed convection in a square cavity. The authors concluded that for small values of Ri, the Nusselt number keeps a minimum value at the beginning of the splitting of flow along the hot wall, this behavior does not happen for high values of Pr. When increasing Ri, flow splitting does not appear along the hot wall and the behavior remains linear. The effect over heat transfer when increasing Pr, in considerably higher than increasing Ri.

Regarding turbulent regime studies, Nielsen et al. [12–16] have been pioneers on using Computational Dynamic Fluids to carry out simulations on cavities representing rooms. Most of Nielsen's et al research work is focused on characterizing the aerodynamic influence and geometry parameter related to the inlet air, dimensions of the cavity and inlet and outlet locations over the flow patterns and ventilation efficiency on mixed convection. In [16], Nielsen states that it is important to consider quality and credibility on predictions based on Computational Dynamic Fluids in ventilated cavities, due to care should be taken when implementing the boundary conditions at the inlet of air flow, and when turbulence models are applied. Sakamoto and Matsuo [17] evaluated the behavior of two different models on turbulence to predict recirculation in ventilated cavities, the authors concluded that the turbulence standard model k–ε is the adequate to simulate air flow inside rooms. Later Davidson and Olsson [18] carried out a numerical analysis on flows affected by buoyancy force in ventilated cavities. The authors concluded that air age and purge velocity are necessary parameters to characterize performance of ventilated rooms. In the same way Chen [19,20] carried out a study of mixed convection in ventilated cavities by the use of commercial software PHOENICS. In [19], Chen compared his numerical results with the experimental results given by [14], from which he concluded that turbulence intensity is lower than the reported by the experiment, which means that turbulence is underestimated. In [20], Chen evaluated the performance of five models k–ε, where a prediction on average velocity over the five models was satisfactory, but a prediction on turbulent velocity did not agree with experimental results. This is attributable to the fact that the turbulent models applied on simulations consider turbulence as isotropic, and in the presence of non-isotropic turbulence in the inlet air flow the models fail. The standard model k–ε and RNG remain stable during the calculations. Rees et al. [21] presented a transient study on a room with mechanical ventilation and an inside heat source. Inlet and outlet air gaps location were considered to be on the lower and upper side of the vertical walls respectively. Numerical results showed that complex oscillations on the heat sources occur, which increase recirculation inside the room. More recently Moureh and Flick [22] presented results on an experimental and numerical study, where characteristic velocities in ventilated cavities as function of the location of the inlet and outlet, both on the same wall, is analyzed. This study showed that, location of the inlet aside the wall prevents separation of the inlet flow. This issue improves homogeneous ventilation and allows a uniform distribution of environmental parameters inside the cavity such as temperature and contaminants concentration.

According to the literature review, there exist scarce research works on ventilated rooms with conjugated heat transfer involving conduction and mixed convection in turbulent flow regime; therefore, there is a need to get a deeper knowledge on thermal load gains inside rooms with adequate ventilation. The aim of this research work is to carry out a numerical analysis on conjugated heat transfer (conduction and convective heat transfer) inside a room with a heat conductive wall, and to analyze the effect of positioning in different places the outlet of air, the type and width of material used on the conductive wall and the velocity of supplied air, in order to determine the best configuration for ventilation based on the temperature distribution effectiveness index and the heat gains inside the room. The room is modeled as a square cavity and the conductive wall is set as opaque. For this study, four configurations for the outlet of air were considered: (A) Outlet on the upper side of the left vertical wall, (B) Outlet on the left side of the upper horizontal wall, (C) Outlet at the centre of the upper horizontal wall, (D) Outlet on the right side of the upper horizontal

wall. Two construction materials for the conductive wall are considered: construction brick and adobe block. Velocities of supplied air are set as a function of the Reynolds number between 2×10^3 and 4×10^4.

2. Physical model

The physical model is a two dimension cavity, taking into account that the dimension in z direction is much longer than the other two. Initially, the air inside the cavity is at constant temperature, the right vertical wall is opaque and submitted to a constant heat flux normal to the outside surface, where heat is conducted to the inside surface of the wall producing a temperature gradient between this surface and the air inside the cavity, as the outside surface and the ambient air does, causing radiative and convective heat exchange with the outside ambient. The right vertical wall has a gap in its lower side for the inlet of air. The left side vertical wall and the horizontal walls are considered adiabatic. The outlet position is set for four configurations as shown in Fig. 1a.

3. Mathematical model

3.1. Convective model

The governing equations for convective heat transfer inside a ventilated cavity are mass, momentum and energy equations, averaged in time:

$$\frac{\partial(\rho u_i)}{\partial x_i} = 0 \tag{1}$$

$$\frac{\partial(\rho u_i u_j)}{\partial x_j} = -\frac{\partial P}{\partial x_i} + \frac{\partial}{\partial x_j}\left[\mu\left(\frac{\partial u_i}{\partial x_j} + \mu\frac{\partial u_j}{\partial x_i}\right) - \overline{\rho u_i' u_j'}\right] - \rho g_i \beta (T - T_\infty) \tag{2}$$

$$\frac{\partial(\rho u_j T)}{\partial x_j} = \frac{1}{Cp}\frac{\partial}{\partial x_j}\left(\lambda\frac{\partial T}{\partial x_j} - \rho Cp\overline{u_j' T'}\right) \tag{3}$$

where the turbulence stress and turbulent heat flux vector are approximated as:

$$\overline{\rho u_i' u_j'} = -\mu_t\left[\frac{u_i}{\partial x_j} + \frac{\partial u_j}{\partial x_i}\right] + \frac{2}{3}\rho\kappa\delta_{ij} \tag{4}$$

$$\rho C_p \overline{u_i' T'} = -\frac{\mu_t}{\sigma_T}\frac{\partial T}{\partial x_i} \tag{5}$$

and turbulent viscosity (μ_t) is related to turbulent kinetic energy (k) and to the turbulent kinetic energy dissipation (ε) by the Kolmogorov–Prandtl empirical expression as:

$$\mu_t = C_\mu \frac{\rho k^2}{\varepsilon} \tag{6}$$

To enclose the turbulence mathematical problem, the turbulent kinetic energy (k) and the turbulent kinetic energy dissipation (ε) are required [23]:

$$\frac{\partial(\rho u_i k)}{\partial x_i} = \frac{\partial}{\partial x_i}\left[\left(\mu + \frac{\mu_t}{\sigma_\kappa}\right)\frac{\partial k}{\partial x_i}\right] + P_k + G_k - \rho\varepsilon \tag{7}$$

$$\frac{\partial(\rho u_i \varepsilon)}{\partial x_i} = \frac{\partial}{\partial x_i}\left[\left(\mu + \frac{\mu_t}{\sigma_\varepsilon}\right)\frac{\partial \varepsilon}{\partial x_i}\right] + C_{\varepsilon 1}[P_k + C_{\varepsilon 3} G_k]\frac{\varepsilon}{k} - C_{\varepsilon 2}\frac{\rho\varepsilon^2}{k} \tag{8}$$

where P_k and G_k are the sheer production of turbulence kinetic energy and the buoyant production/destruction of turbulence kinetic energy respectively. The coefficient values for κ–ε turbulence model are: $C_\mu = 0.09$, $C_{1\varepsilon} = 1.44$, $C_{2\varepsilon} = 1.92$, $\sigma_\kappa = 1.0$, $\sigma_\varepsilon = 1.3$ and $C_{3\varepsilon} = \tanh|v/u|$.

The velocity boundary conditions are fixed as zero over the solid surfaces. Velocity at the gap of the inlet is $u = u_{\text{in}} = f(Re)$ and $v_{\text{in}} = 0$ and at the gap of the outlet $\partial u/\partial n = 0$ and $\partial v/\partial n = 0$, where n is direction normal to the outlet surface. Thermal boundary conditions are: $\partial T/\partial n = 0$ for the adiabatic walls, temperature at the inlet of air as $T = T_{\text{in}} = 24\,^\circ\text{C}$, boundary temperature at the gap for the outlet of air as $\partial T/\partial n = 0$ and boundary condition for the interaction of the opaque wall with the fluid inside the cavity is obtained by a thermal balance as:

$$q_{\text{cond-m}} = q_{\text{conv-int}} \tag{9}$$

Boundary conditions for turbulent quantities (ε, k) are: $k_{\text{in}} = 1.5(0.04u_{\text{in}})^{2.0}$ and $\varepsilon_{\text{in}} = (k_{\text{in}})^{0.5}/(0.1L_{\text{in}})$ at the inlet gap, $\partial\varepsilon/\partial n = 0$ and $\partial k/\partial n = 0$ at the outlet gap and over the solid surfaces the fix values for $\varepsilon and k$ proposed by [23].

3.2. Conductive model

Two dimension governing equations for heat conduction through the vertical wall to the right is:

$$\frac{\partial}{\partial x}\left(\lambda_m\frac{\partial T_m}{\partial x}\right) + \frac{\partial}{\partial y}\left(\lambda_m\frac{\partial T_m}{\partial y}\right) = 0 \tag{10}$$

where, λ_m is thermal conductivity of the wall and, T_m is temperature on the wall.

The boundary conditions are adiabatic horizontal surfaces and a constant heat flux over the outside surface of the vertical wall to the right as

$$Q = q_{\text{cond-m}} + q_{\text{conv-ext}} + q_{\text{rad-ext}} \tag{11}$$

Fourier's Law is applied on Eq. (11) to define $q_{\text{cond-m}}$, for the second right hand term $q_{\text{conv-ext}}$ Newton's cooling Law is used, and for the last term of the equation $q_{\text{rad-ext}}$ the Stefan–Boltzmann Law is applied.

The boundary condition on the inside surface of the opaque wall is the same as Eq. (9).

4. Thermal parameters

4.1. Temperature distribution effectiveness

Temperature distribution effectiveness is a parameter related to the way in which temperature pattern is distributed along the cavity. Awbi defines this parameter as a function of the following variables [2]:

$$\overline{\varepsilon_t} = \frac{T_{\text{out}} - T_{\text{in}}}{T_{\text{average}} - T_{\text{in}}} \tag{12}$$

where: T_{out} is the air average temperature at the outlet gap, T_{average} is the air average temperature all over the cavity and T_{in} is the air average temperature at the inlet gap.

4.2. The Nusselt number on the heat conductive wall

The average Nusselt number is a parameter to quantify total heat transfer inside the cavity, and is defined as a ratio of the convection heat transfer over the conduction heat flux through the cavity as

$$Nu = \frac{1}{q_{\text{ref}}}\int_{L_{\text{in}}}^{H} q_{\text{conv-int}}\,dy = \frac{-\lambda}{q_{\text{ref}}}\int_{L_{\text{in}}}^{H}\frac{\partial T}{\partial x}\,dy \tag{13}$$

where: $q_{\text{conv-int}}$ is the heat transfer inside the cavity from the conductive wall, q_{ref} is the conduction heat flux through the cavity given by $q_{\text{ref}} = \lambda(T_4 - T_2)/W$, with T_4 as the average temperature on the inside surface of the conductive wall and T_2 as the average temperature on the vertical wall to the left of the cavity.

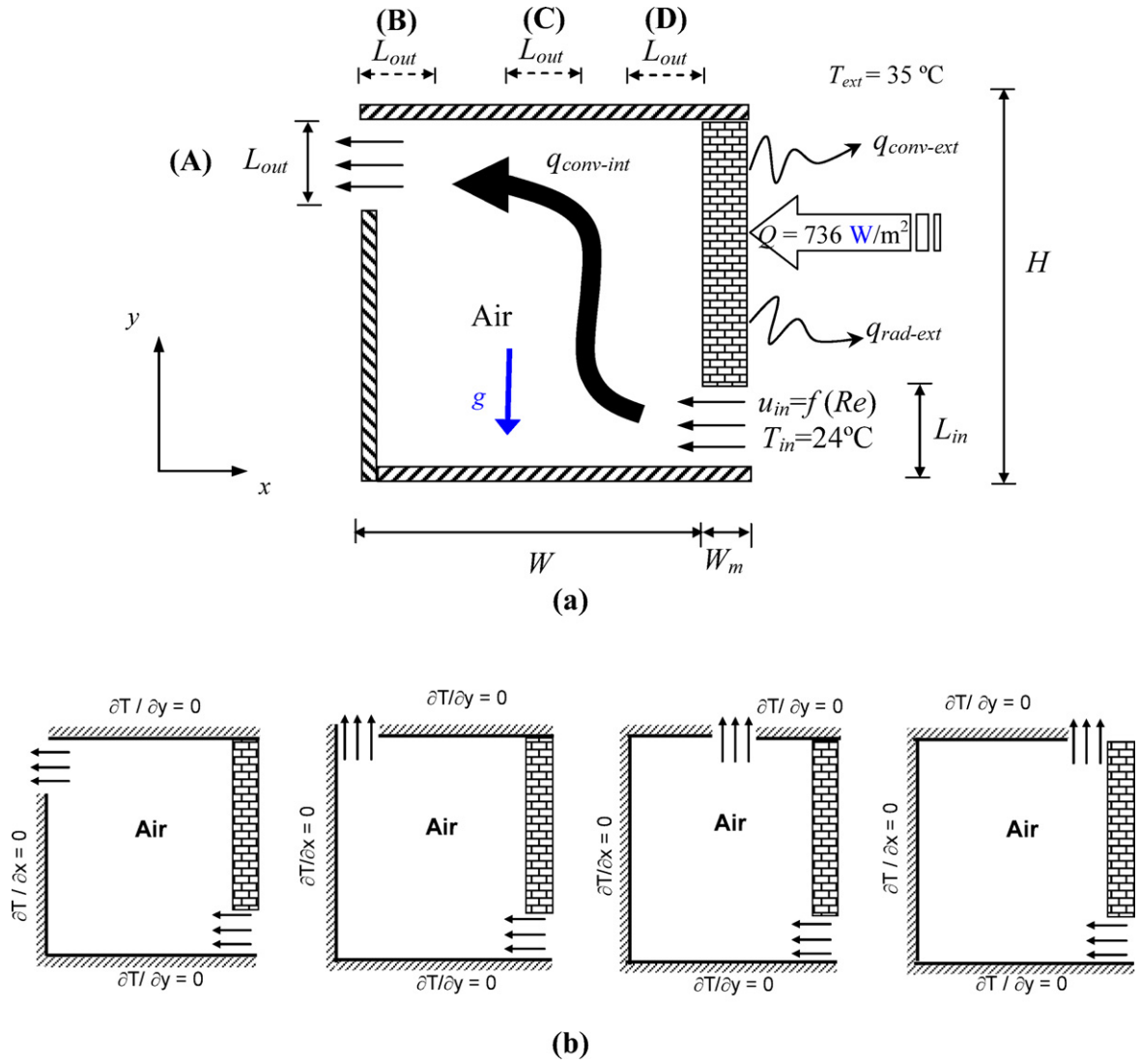

Fig. 1. Ventilated cavity: (a) Physical model and (b) cases of study.

5. Methodology for the numerical solution

The governing equations describing the flow and heat transfer were discretized by the finite volume technique [24]. In order to implement the numerical algorithm, the governing equations can be represented by the following general equation of convection–diffusion:

$$\frac{\partial}{\partial x_j}(\rho u_j \phi) = \frac{\partial}{\partial x_j}\left(\Gamma \frac{\partial \phi}{\partial x_j}\right) + S_\phi \tag{14}$$

Integration of Eq. (14) over the corresponding finite volume and substitution of every term by discrete values of ϕ in the nodal points gives the following algebraic equation for every nodal point:

$$a_P \phi_P^{n+1} = \sum_{\mathrm{nb}=E,O,N,S} a_{\mathrm{nb}} \phi_{\mathrm{nb}}^{n+1} + b^n \tag{15}$$

Where n is the iteration number, nb are the neighbor coefficients, b is the source term and ϕ represents the discrete value of the dependent variable over the control volume.

The position of the grid nodes is calculated using a stretching function so that the nodes are closer to each other near the walls of the cavity. The velocity components are calculated at a staggered grid while the scalar variables are calculated at the main grid (not staggered). For coupling of mass and momentum equations, the SIMPLEC algorithm was used [25]. Convective terms were approached by the upwind scheme and diffusive terms by the centered scheme. The resulting system of algebraic equations was solved by the Line By Line (LBL) iterative method. The convergence criteria was 10^{-8} for the residual of each equation. An independency of mesh analysis was carried out, for a mesh size from 91×71 to 141×121 with an increment of 10 computer nodes; it was found that a mesh size of 131×111 nodes was satisfactory, with a maximum deviation of 1% for the average Nusselt number, the maximum velocity components and the average temperature. The discretization for the conductive wall was always 20 nodes in the horizontal direction for all the meshes.

In order to validate the computer code, the problem proposed by [14], was solved as described as follows. The problem is defined by a ventilated cavity under isothermal conditions and turbulent flow regime with inlet and outlet of air on the vertical walls. The cavity is $H = 3.0$ m height and $W = 9.0$ m width, the incoming air is forced to go through the upper side of the left wall and leaves the room by the lower side of the right wall, all the walls were considered adiabatic. The inlet gap is $0.056 * H$ and the outlet gap is $0.16 * H$. Fig. 2 shows results for the non-dimensional velocity horizontal component u^* for four different non-dimensional sections of the cavity. Figs. 2a and 2b show velocities along y^* on the positions $x^* = 1.0$ and $x^* = 2.0$, in the same way, Figs. 2c and 2d show velocities along x^* on the position $y^* = 0.972$ and

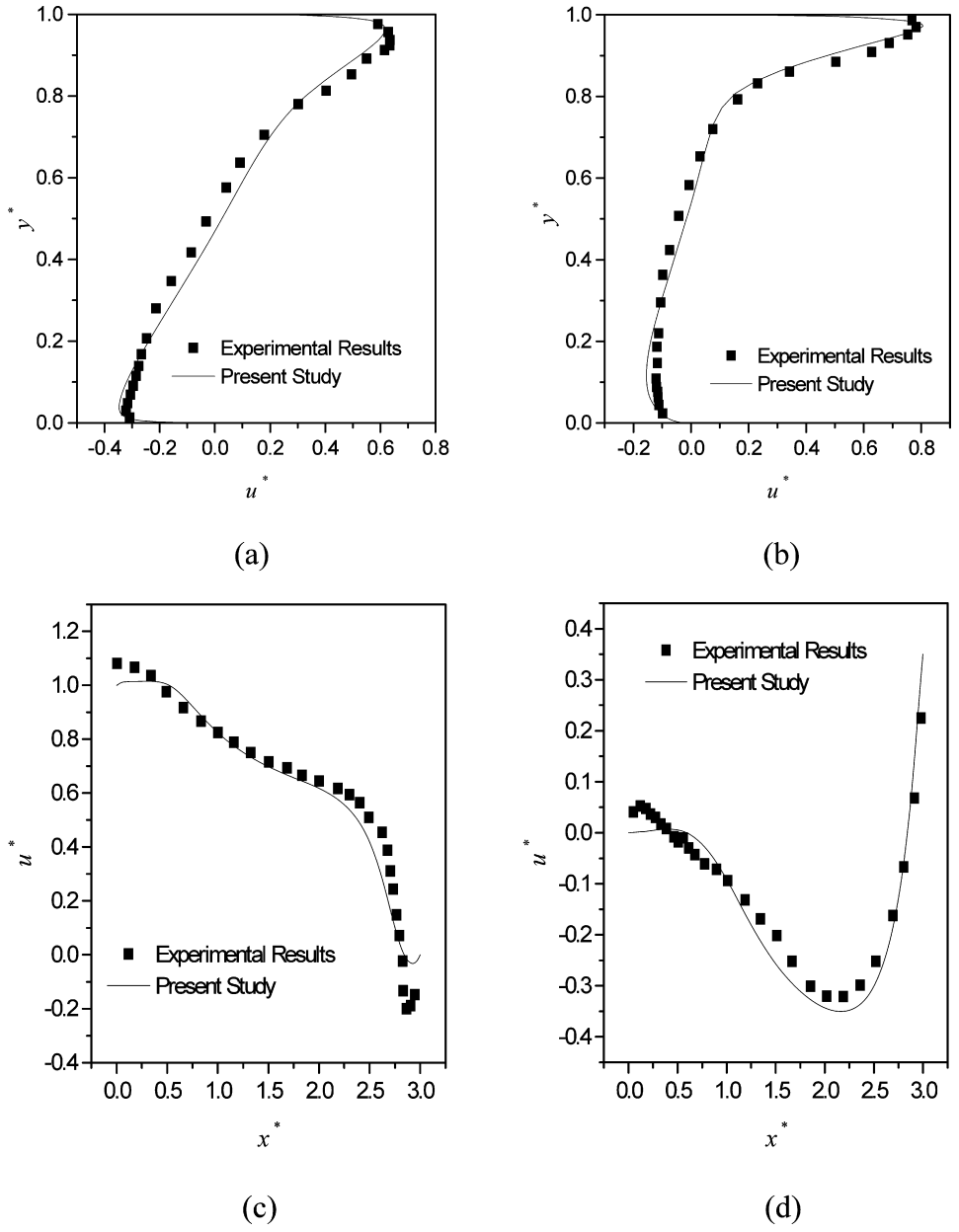

Fig. 2. Comparison of the u^*-velocity between Nielsen (1990) and the present study in: (a) $x^* = 1.0$, (b) $x^* = 2.0$, (c) $y^* = 0.972$, and (d) $y^* = 0.028$.

$y^* = 0.028$. From both figures can be concluded that numerical results have an acceptable qualitative approximation, and from a quantitative point of view, the maximum error compared to the experimental results is 16.14%.

6. Results and discussion

6.1. Parameter of study

For this study an actual size room cavity 3.0×3.0 m^2 was considered. The inlet and outlet of air are 0.3 m height, the same size as the air conditioning diffusers. Supplied air temperature was set at 24 °C and the outside ambient temperature at 35 °C; the convective coefficient (h_{ext}) was 6.8 W/m^2 K and 0.88 for the emissive coefficient of the white paint for the outside surface of the conductive wall. The heat flux on this wall has a constant value of 736 W/m^2 [26].

In order to establish the best configuration for ventilation based on the temperature distribution effectiveness and to obtain comfort temperature inside the cavity, an analysis was carried out, taking into account the air outlet position. Four configurations were considered: (A) Outlet on the upper side of the left vertical wall, (B) Outlet on the left side of the upper horizontal wall, (C) Outlet at the centre of the upper horizontal wall, (D) Outlet on the right side of the upper horizontal wall as shown in Fig. 1b. Another important parameter is the incoming air velocity, which varied from 0.1 to 2.0 m/s. The minimum velocity of 0.1 m/s is equivalent to remove inside air at a rate of 36 m^3/hr per person, and 2.0 m/s as the maximum velocity for air conditioning diffusers, as recommended by ASHRAE Standard 55 [1]. Six values for the

Table 1
Physical properties of Adobe block and Construction brick.

Material	ρ_m (kg/m^3)	λ_m (W/m K)	Cp_m (J/kg K)
Adobe block	1620	0.49	1240
Construction brick	1800	0.72	829

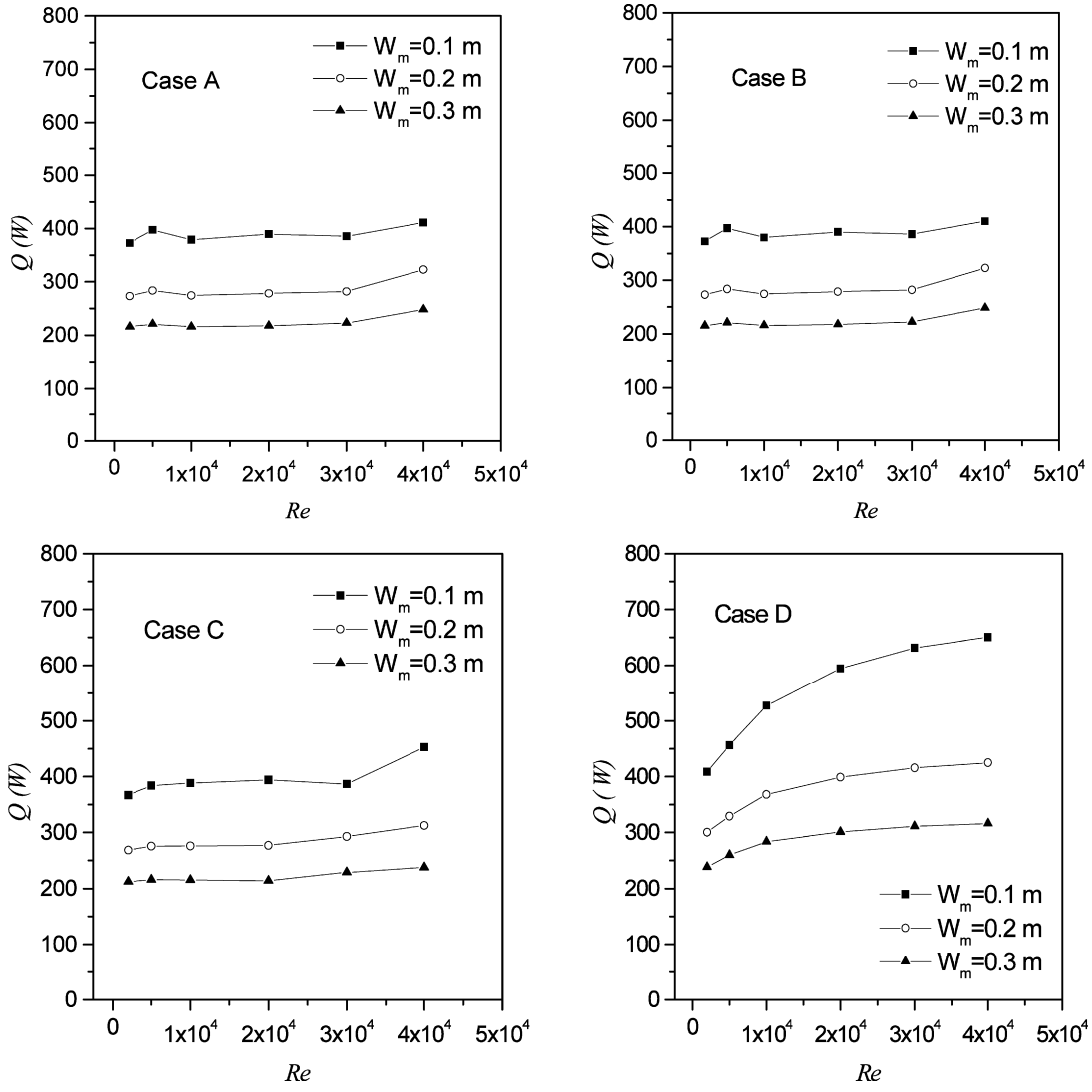

Fig. 3. Wall width effect on the construction brick conductive wall.

incoming air velocity were chosen: 0.10, 0.25, 0.52, 1.0, 1.54 and 2.0 m/s, and their corresponding Reynolds number are 2×10^3, 5×10^3, 1×10^4, 2×10^4, 3×10^4 and 4×10^4. Thermal load gains is strongly related to the type of material and width of the conductive wall, so two types of materials were chosen: construction brick and adobe block due to they are representative as construction materials, and 0.1, 0.2 and 0.3 as representative width of walls. Physical properties values for both materials are shown in Table 1.

6.2. Effect of type of material and width of the conductive wall for the ventilated cavity

Before analyzing the temperature distribution effectiveness inside the cavity, it is important to determine the effect that the construction material and the width of the wall have on reducing thermal load gains. This behavior depends strongly on the physical properties.

Fig. 3 shows the heat flow inside the cavity using construction brick for each outlet position and width over the entire Reynolds interval. From it can be seen values of heat flow between 200 and 700 W. The behavior of heat flow between 200 and 400 W look similar for cases A, B and C; but for case D, heat flow reaches a maximum of 700 W, due to the flow pattern formed for this case [27]. Regarding to the wall width, it can be seen that as the width increases the heat flow to the inside decreases; the same behavior was observed for the adobe block, so it can be concluded from the three cases that the 0.3 m width is more appropriate to reduce thermal loads.

In order to analyze the material efficiency on reducing thermal load gains, both materials, construction brick and adobe block, were compared using a 0.3 m width for the wall on all the four outlet position configurations. Results can be seen in Fig. 4, where the adobe block seems to have the best performance on reducing thermal load gains to the inside of the cavity, this behavior is attributable to the physical properties of each material. Specific heat for the adobe is higher than for the construction brick, this property gives the adobe a major capacity as a heat storage, and not letting go through heat. On the other hand, thermal diffusivity is higher for the construction brick, which makes it an easy media to release heat to the inside of the cavity. The average flow rate for cases A, B and C are 225 W for the construction brick and 175 W for the adobe block; for case D, values are sensibly higher.

To conclude, the adobe block wall with a 0.3 m width has the best performance for all the configurations (A, B, C, and D) on reducing thermal load gains, this makes easier the effort to remove heat by convection.

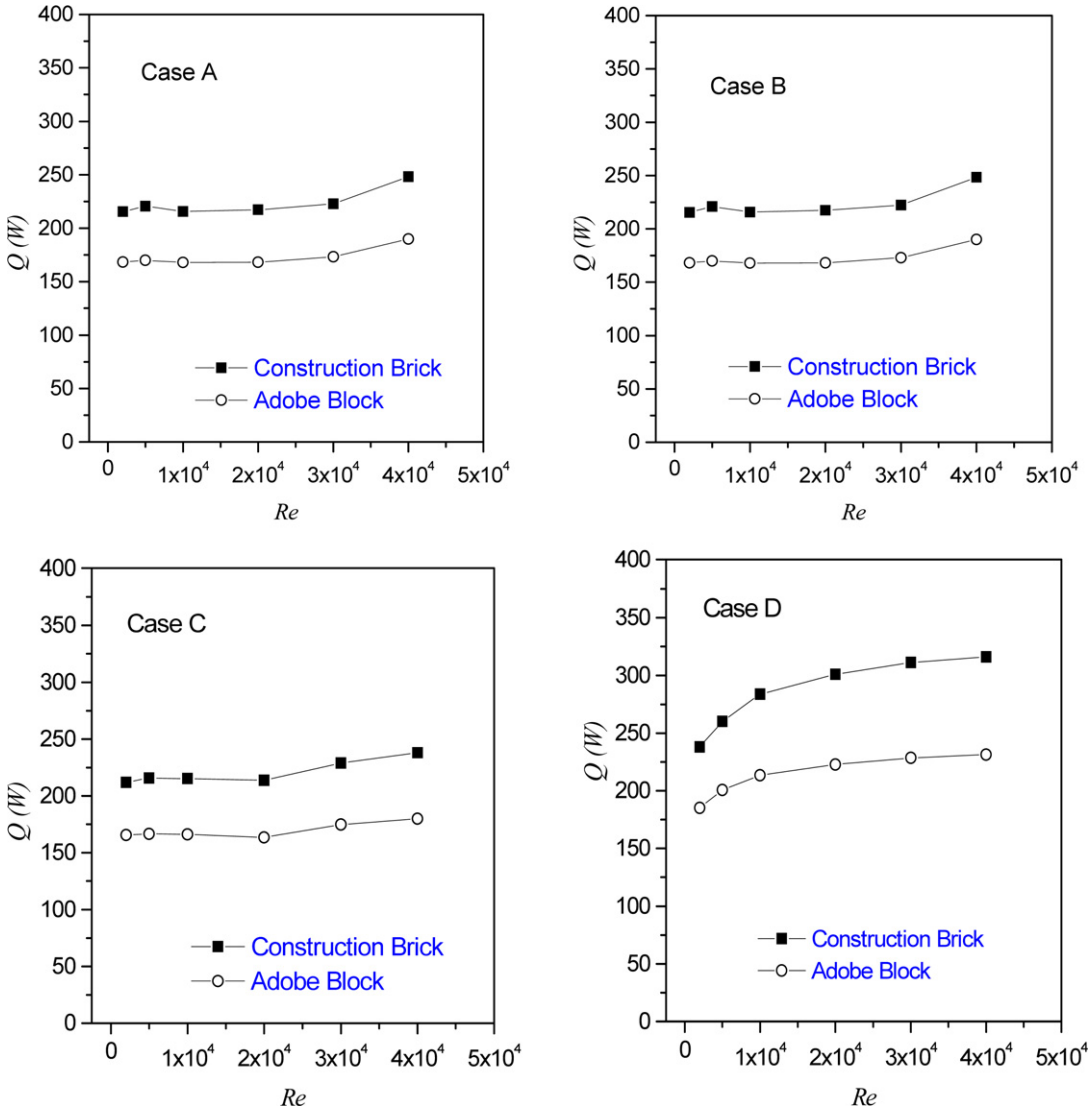

Fig. 4. Effect of the type of material for a width of 0.3 m of wall.

6.3. *Flow patterns for a Reynolds number of* 2×10^4

Two important aspects to be taken into account are: air velocity and temperature distributions inside the cavity, the called flow patterns, due to the thermal behavior shall strongly depend on them. Fig. 5 shows the streamlines for each of the configurations with a Reynolds number of 2×10^4, and for a 0.3 m width Adobe wall, that according to the previous section it corresponds to the case for which the heat gain was the lowest. For all the cases, it can be observed from Fig. 5 that the main current flow moves over the lower part of the cavity until it collides on the wall opposite to the air inlet, and then it flows along this wall up to the air outlet. Two circulating vortexes show up for cases A, B and C, and for case D they become a unified vortex. From the two vortexes cases, the one next to the main flow rotates the main current wise; opposite to it, the other vortex rotates in the same direction as the upward flow does, along the conductive wall. On configuration D, where the vortexes become a unified vortex, it rotates counterclockwise. In general, the "L" shape flow patterns for cases A and B, and the "C" shape patterns for cases C and D, all of them with a vortex next to the conductive wall represent an undesirable state when one wants to achieve an adequate temperature distribution or when heat has to be removed focused on achieving thermal comfort. The corresponding isothermals are shown in Fig. 6, from which it can be observed that the isothermals show a tendency to form lines that run from the inlet to the outlet, for cases A and B they highlight a diagonal which divides the cavity, for case C they run towards the center of the upper adiabatic wall, and for case D they run towards a section next to the wall. The patterns show two perfectly defined zones inside the cavity, the cold zone on the left hand of the cavity with temperatures from 24 to 25.5 °C and the hot zone on the right hand with temperatures from 26 to 31 °C.

6.4. *Temperature distribution effectiveness for the cavity*

Fig. 7 shows temperature distribution effectiveness ($\overline{\varepsilon_t}$) for a cavity with a 0.3 m width adobe conductive wall, tested on the four configurations of the outlet position and their corresponding Reynolds numbers. From this figure can be seen that cases A, B and C present low effectiveness indexes and case D high indexes. The Reynolds number also has a significant effect on case D, where the highest effectiveness of all can be seen for *Re* from 2×10^3 to 1×10^4, for higher values of *Re*, effectiveness gradually decreases to a constant value. From this result can be concluded that the best values for the incoming air velocities for a system with the previously defined characteristics are between 0.1 and 0.5 m/s; higher values for velocity only increase the energy consumption with-

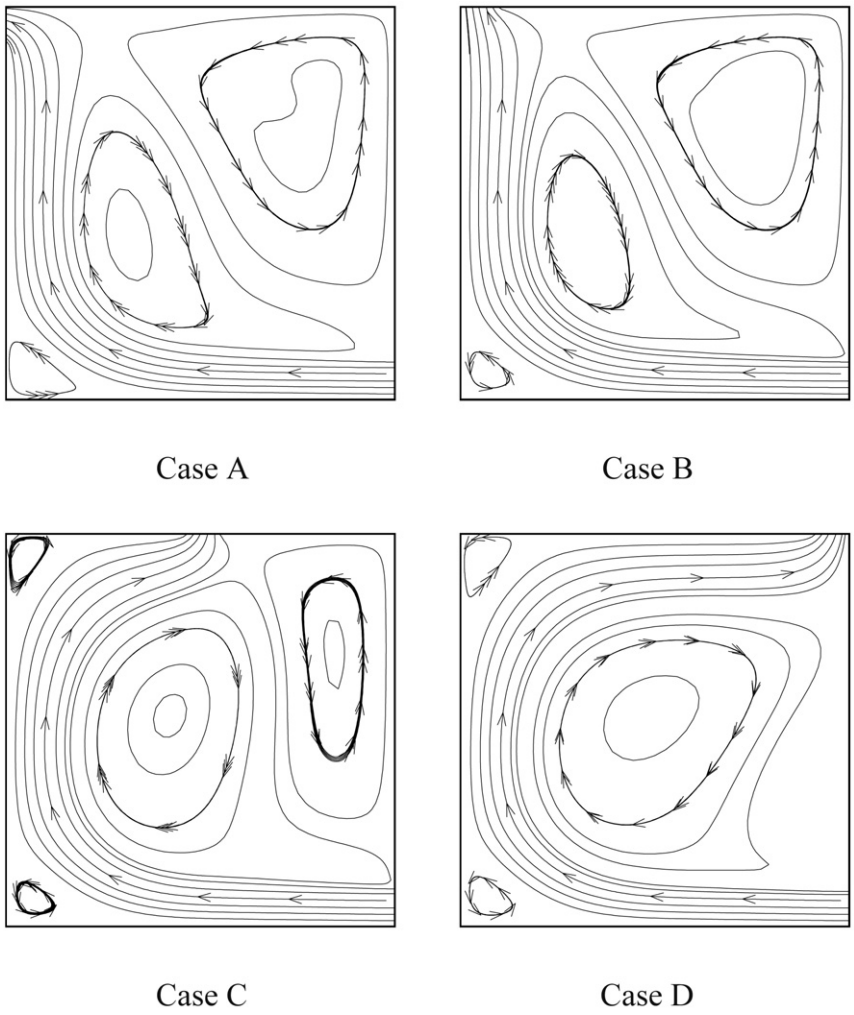

Fig. 5. Streamlines for a $Re = 2 \times 10^4$.

out improving temperature distribution effectiveness. This phenomenon is due to that when increasing the incoming air flow velocity, a maximum optimal value is reached and the main incoming stream shows a tendency to flow farther away the conductive wall surface without interacting with the hot air area. Table 2 shows the average temperature for the four cases; it can be seen that the lowers average temperature are obtained on case D, and from a $Re = 1 \times 10^4$ this temperature shows an almost constant behavior and gradually tends to the same value of the incoming air temperature. Therefore, configuration D represents the best configuration with the highest temperature distribution effectiveness index between a *Re* from 2×10^3 to 1×10^4; the obtained average temperatures (24.69–26.23 °C) fall between the interval defined by [1] as a standard temperature for human comfort (22.7–27.77 °C).

ASHRAE Standard 55 [1] states that velocity inside a room should have a maximum value of 0.1 m/s in winter and 0.25 m/s in summer. This criterion is based on experimental studies carried out on people submitted to an air flow 30 cm away from their face and the back of the neck; the air flow velocity was characterized as agreeable to disagreeable according to their own sensations. For this reason, this velocity should be found at a person average height between 1.0 and 2.0 m, for ventilation analysis purposes.

Fig. 8 shows the resulting speed for D case of study for Reynolds numbers of de 2×10^3, 5×10^3 and 1×10^4. The resulting velocity along the width is presented for different heights of 1.01, 1.50 and 2.05 m. For $Re = 2 \times 10^3$, a stagnation inside the cavity zone can be observed, where velocity is near to zero on the left side of the cavity, but next to the right side velocity is near to 0.35 m/s due to the fact that air flow concentrates mainly in that area. It can be concluded that, for this case ($Re = 2 \times 10^3$) velocities stated by [1] are valid only from the center of the cavity to the vertical right wall. For $Re = 5 \times 10^3$, the highest velocity values are close to the vertical walls and they become smaller at the center, but the average velocity is 0.12 m/s. Similar results are obtained for $Re = 1 \times 10^4$, with an average value of 0.17 m/s. To conclude, although results for $Re = 2 \times 10^3$ gives a relatively good temperature distribution, from a velocity point of view it does not result adequate due to the stagnation of air zone formed when velocities are close to zero. For that reason, an optimal interval for Reynolds number is given between 5×10^3 and 1×10^4, with average velocities from 0.12 to 0.17 m/s respectively, this fulfills ASHRAE Standard 55 requirements [1].

The streamlines for configuration D is shown in Fig. 9, as a function of the Reynolds number. In general, a main vortex can be seen which increases it size as *Re* does, in particular it can be observed that for a $Re \leqslant 1 \times 10^4$ the main vortex is completely surrounded by the main stream of the flow, and for these cases the main stream of the flow interacts with the inside surface of the conductive wall. On the other hand, for a $Re > 1 \times 10^4$, the main vortex has increased its size significantly which has allowed it to interact with the conductive wall; and it is the size of the vortex itself that prevents the main stream to interact with the conductive wall.

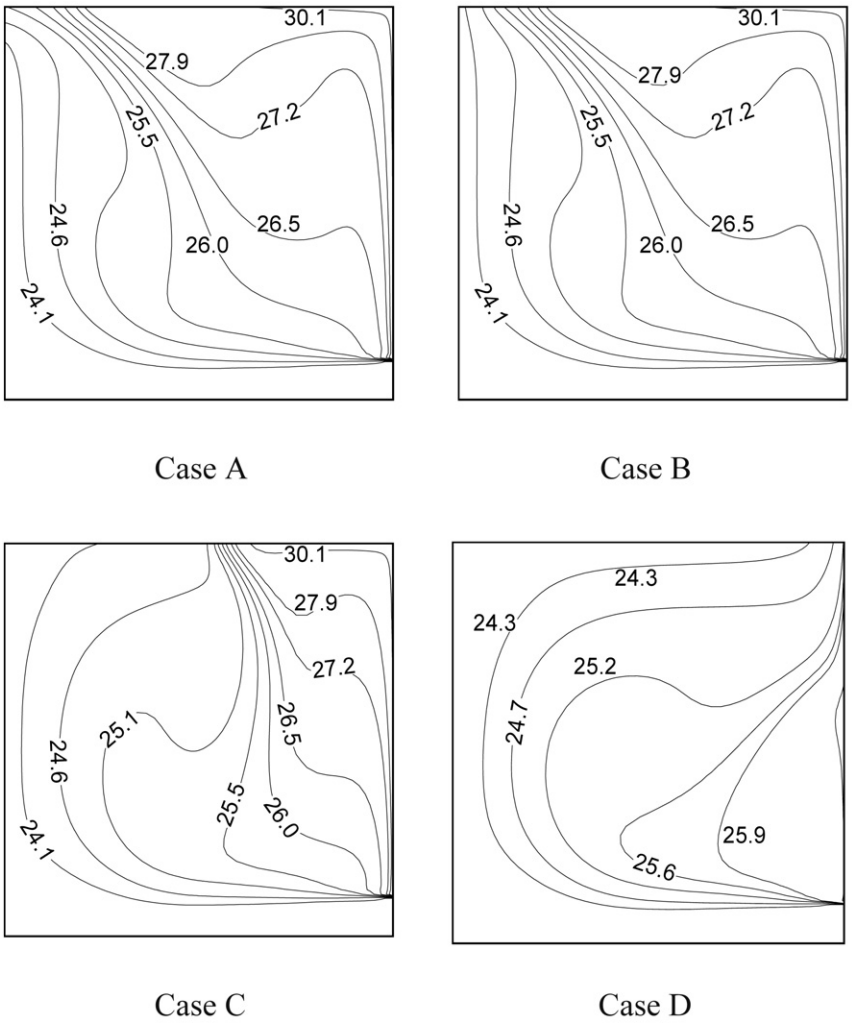

Fig. 6. Isothermal (°C) for a $Re = 2 \times 10^4$.

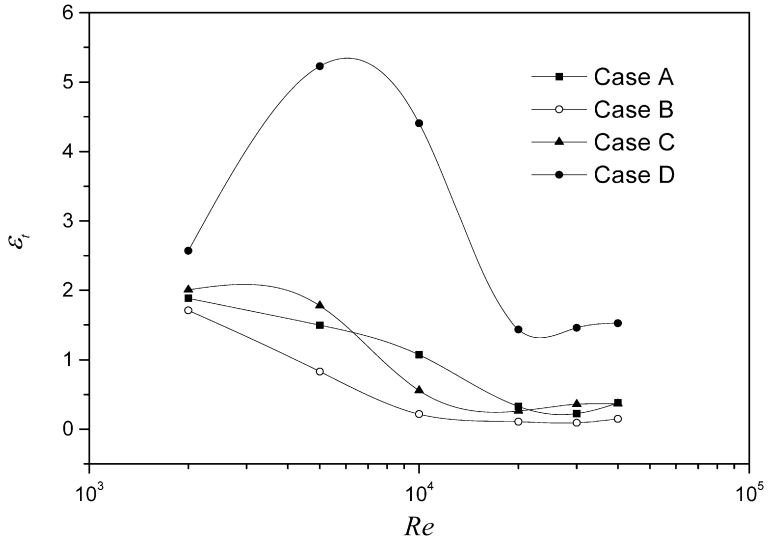

Fig. 7. Temperature distribution effectiveness index.

The corresponding isothermals are shown in Fig. 10, from which it can be seen that for a $Re = 2 \times 10^3$ a stratification zone at the upper half of the cavity shows up causing an almost null movement of the fluid with high temperatures in this region (higher than 24 °C). For the rest of the Reynolds numbers, in most of the cavity the following temperature intervals can be

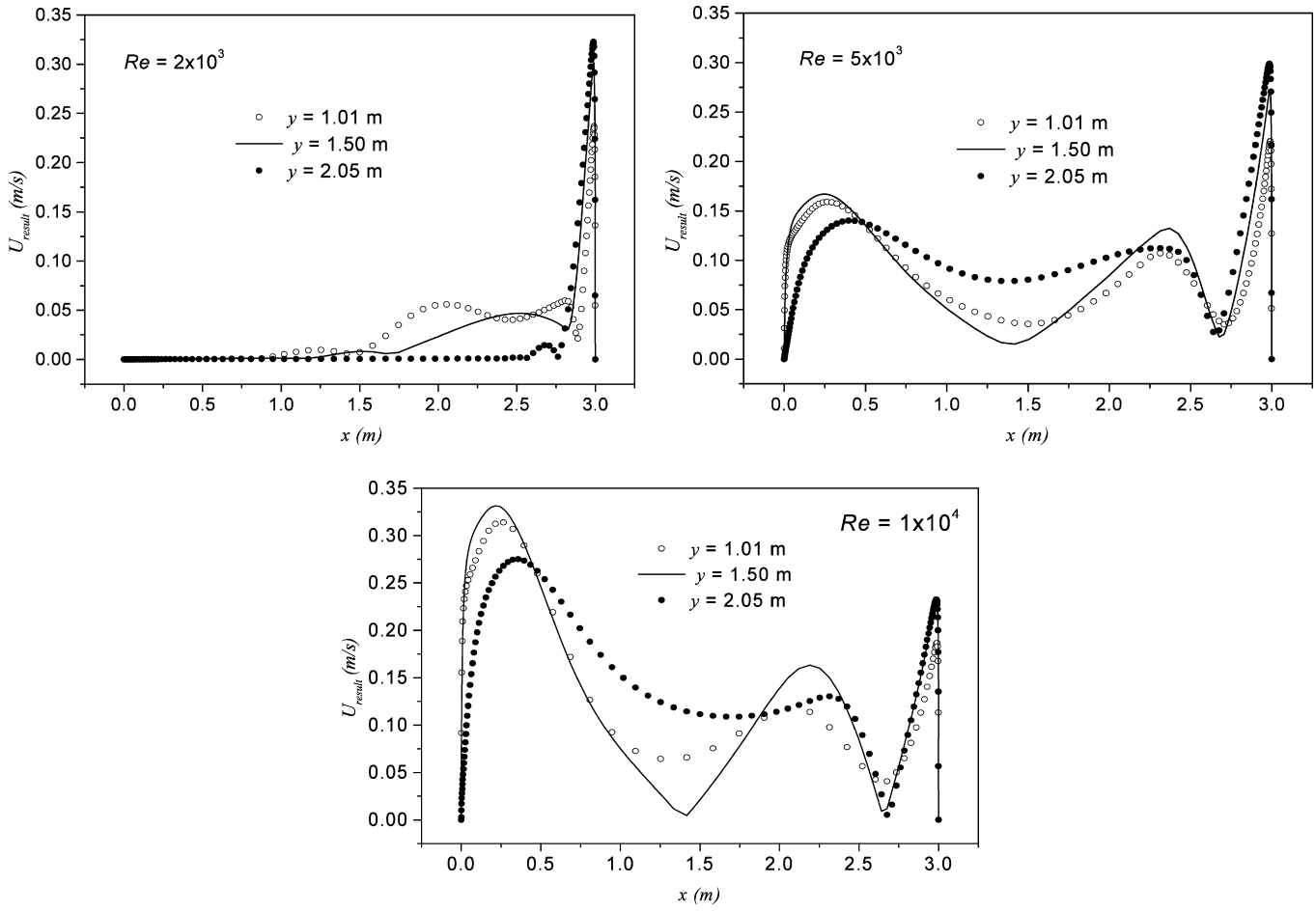

Fig. 8. Resulting velocities for different heights of the cavity.

Table 2
Average temperature (°C) inside the cavity using adobe block.

Re	Case A	Case B	Case C	Case D
2×10^3	26.87	26.79	26.48	26.23
5×10^3	26.87	25.69	25.13	24.78
1×10^4	26.08	25.84	25.15	24.69
2×10^4	26.43	26.34	25.61	24.61
3×10^4	26.10	26.07	25.01	24.50
4×10^4	25.05	25.08	24.80	24.38

seen: 24.0–24.1 °C ($Re = 5 \times 10^3$), 24.1–24.6 °C ($Re = 1 \times 10^4$), 24.3–25.9 °C ($Re = 2 \times 10^4$), 24.1–24.9 °C ($Re = 3 \times 10^4$) and 24.1–24.8 °C ($Re = 4 \times 10^4$). From these last results, can be concluded that for a $Re = 5 \times 10^3$, 1×10^4 the lowest temperature intervals were obtained, this results is consistent with the values calculated for $\overline{\varepsilon_t}$.

6.5. Nusselt number on the wall for the optimal case

Finally, in order quantify the average heat transfer on the system, the average Nusselt number has to be determined. Fig. 11 shows the behavior of the average Nusselt number (Nu) as a function of the Reynolds number for a cavity with a 0.3 m width adobe block for all the analyzed cases. In general, it can be assessed that the heat transfer is higher for case D regarding to cases A, B and C, this is due to that the obtained inside average air temperature is lower for case D, so a higher temperature gradient between the inside surface of the wall and the air would be present, causing an increased average heat flux. Correlations for the average Nusselt numbers for all the cases were derived using least-square linear regression for a cavity with a 0.3 m width adobe block. The Nu correlations are:

Case A:

$$Nu = 4.91E-16Re^4 - 1.63E-11Re^3 + 1.56E-07Re^2 - 0.0024Re + 487.78 \quad (2.19\%)^*$$

Case B:

$$Nu = 9.07E-16Re^4 - 5.45E-11Re^3 + 1.35E-06Re^2 - 0.0174Re + 549.06 \quad (1.33\%)^*$$

Case C:

$$Nu = -2.44E-15Re^4 + 1.96E-10Re^3 - 4.59E-06Re^2 + 0.0378Re + 402.26 \quad (1.44\%)^*$$

Case D:

$$Nu = 0.0348Re + 454.21 \quad (4.12\%)^*$$

* Maximum deviation in percent respect to the numerical results.

7. Conclusions

In this paper a numerical study of conjugated heat transfer inside a ventilated cavity on turbulent flow regime was presented; where convective heat transfer inside the cavity coupled to heat conduction through an opaque wall was analyzed. Four cases of

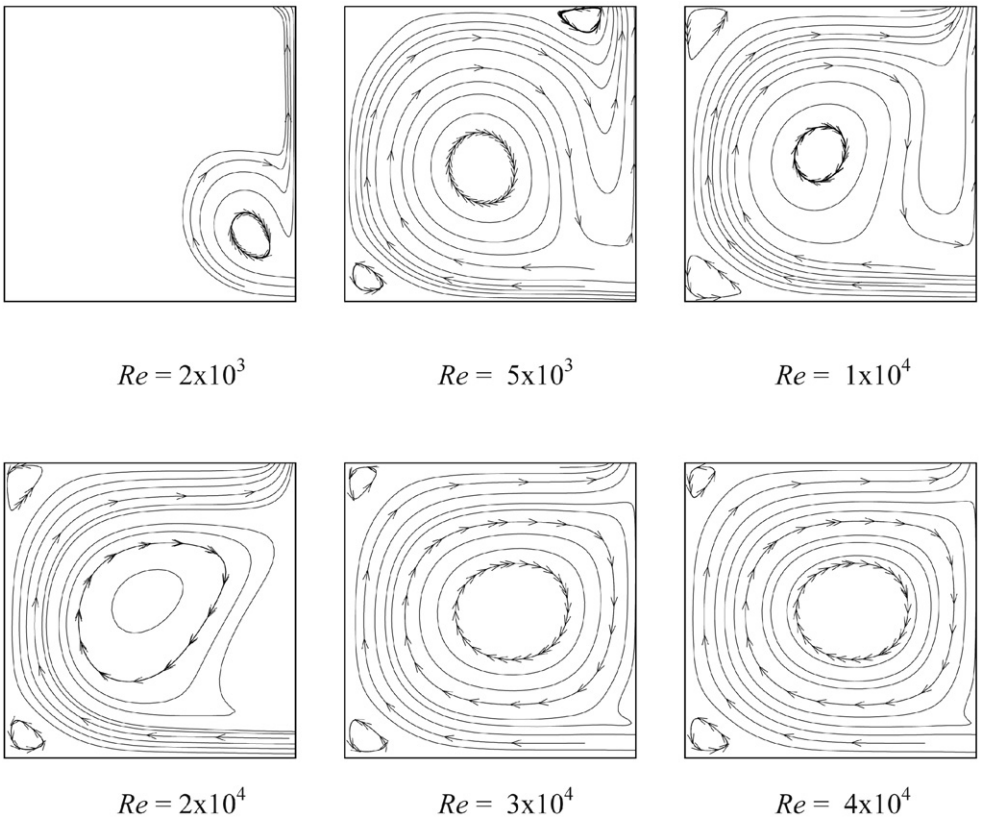

Fig. 9. Streamlines for the case D.

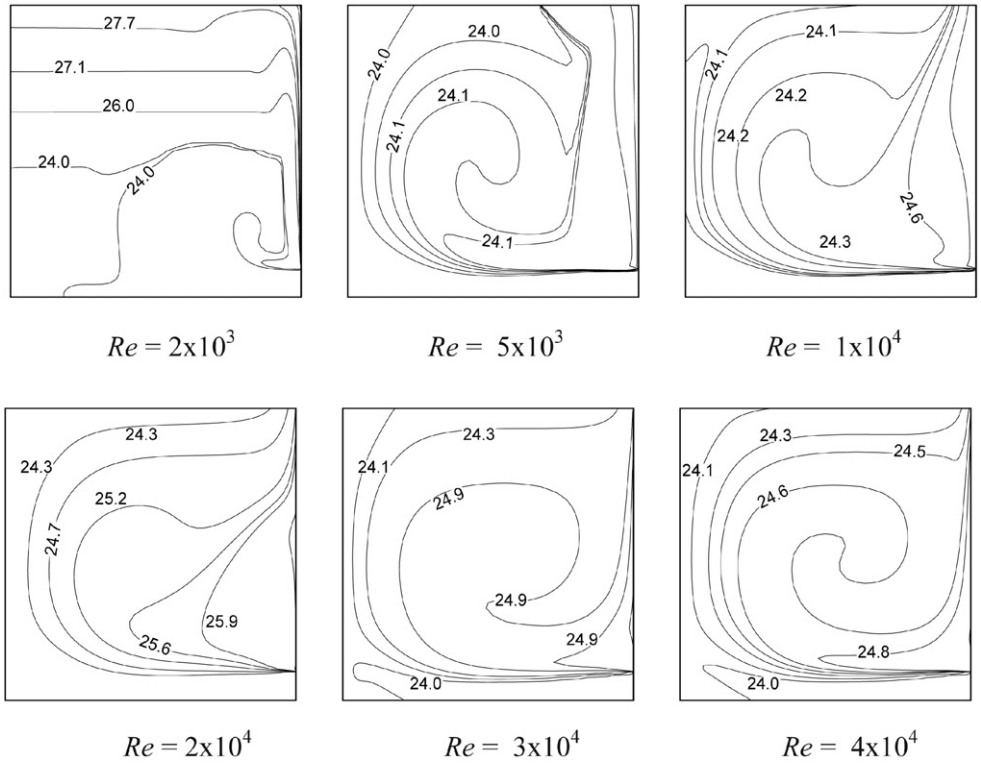

Fig. 10. Isothermal (°C) for the case D.

study were considered for the air outlet position in order to obtain the optimal, based on the temperature distribution effectiveness and the air velocity inside the cavity, according to ASHRAE Standard 55 [1], and to obtain heat gains to the inside.

Base on the results it can be concluded that

1. Regarding the construction material of the conductive wall, adobe block was more efficient than construction brick reduc-

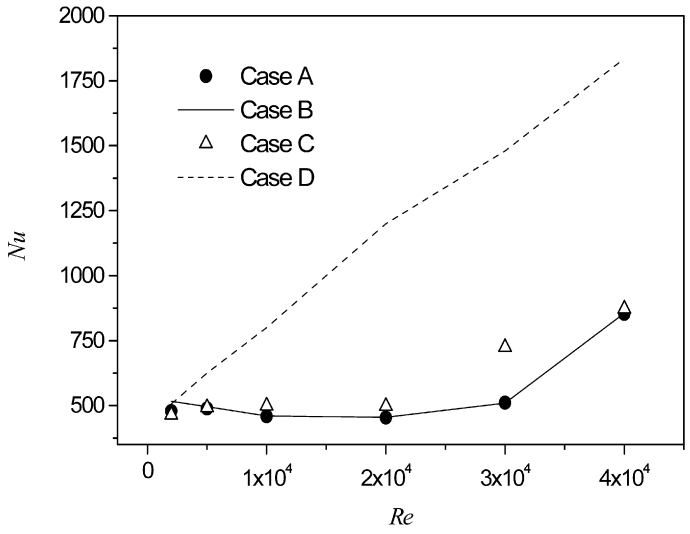

Fig. 11. Average Nusselt number as a function of *Re*.

ing heat gains to the inside of the cavity up to 100 W, due to the specific heat for adobe is higher, which allows it a major heat storage. As heat conducted to the inside proved to be proportionally inverse to the wall width, the 0.3 m width wall was the adequate.

2. From the analysis of temperature distribution effectiveness for a cavity with a 0.3 m width adobe conductive wall, it was found that the D case of study shows the highest effectiveness index. The highest values of temperature distribution effectiveness are for *Re* from 2×10^3 to 1×10^4; nevertheless, results from the analysis of air velocity distribution inside the cavity show that for a *Re* of 2×10^3, velocities are close to zero in more than a half of the cavity making air stagnation to show up, which is not recommendable. On the other hand, air velocity results inside the cavity for a Reynolds of 5×10^3 and 1×10^4, have average values of 0.12 and 0.17 m/s respectively, so according to ASHRAE Standard 55 this is an adequate interval [1].
3. A correlation for the average Nusselt respect to the Reynolds number for each configuration (cases A, B, C and D) was obtained for a cavity with a 0.3 m width adobe conductive wall, showing a maximum percentage difference of 4.12% respect to the numerical results.

References

[1] ASHRAE Standard 55, Thermal environment conditions for human occupancy, 2004.
[2] H. Awbi, Ventilation of building, E & FN Spon, 2003.
[3] E. Papanicolaou, Y. Jaluria, Mixed convection from an isolated heat source in a rectangular enclosure, Numerical Heat Transfer, Part A 18 (1990) 427–461.
[4] E. Papanicolaou, Y. Jaluria, Mixed convection from localized heat source in a cavity with conducting walls, Numerical Heat Transfer, Part A 23 (1993) 463–484.
[5] E. Papanicolaou, Y. Jaluria, Computation of turbulent flow in mixed convection in a cavity with a localized heat source, J. Heat Transfer 117 (1995) 649–658.
[6] A. Raji, M. Hasnaoui, Mixed convection heat transfer in a rectangular cavity ventilated and heated from the side, Numerical Heat Transfer, Part A 33 (1998) 533–548.
[7] A. Raji, M. Hasnaoui, Corrélations en convection mixte dans des cavities ventilées, Rev. Gén. Therm. 37 (1998) 874–884.
[8] A. Raji, M. Hasnaoui, Mixed convection heat transfer in a ventilated cavities with opposing and assisting flows, Engineering Computations 17 (2000) 556–572.
[9] A. Raji, M. Hasnaoui, Combined mixed convection and radiation in ventilated cavities, Engineering Computations 18 (2001) 922–949.
[10] S. Singh, M. Sharif, Mixed convective cooling of a rectangular cavity with inlet and exit openings on differentially heated side walls, Numerical Heat Transfer, Part A 44 (2003) 233–253.
[11] M. Rahman, M. Alim, M. Mamun, M. Chowdhury, A. Islam, Numerical study of opposing mixed convection in a vented enclosure, ARPN J. Eng. and Appl. Sciences 2 (2007) 25–36.
[12] P. Nielsen, A. Restivo, J. Whitelaw, The velocity characteristics of ventilated rooms, J. Fluid Eng. 100 (1978) 291–298.
[13] P. Nielsen, A. Restivo, J. Whitelaw, Buonyancy-affected flows in ventilated rooms, Numerical Heat Transfer 2 (1979) 115–127.
[14] P. Nielsen, Specification of a two dimensional test case, Energy Conservation in Buildings and Community System, Annex 20, Denmark, November, 1990.
[15] P. Nielsen, Description of supply openings in numerical models for room air distribution, ASHRAE Transactions 98 (1992) 963–971.
[16] P. Nielsen, Computational fluids dynamics and room air movement, Indoor Air 14 (2004) 134–143.
[17] Y. Sakamoto, Y. Matsuo, Numerical predictions of three-dimensional flow in a ventilated room using turbulence models, Appl. Math. Modelling 4 (1980) 67–72.
[18] L. Davidson, E. Olsson, A numerical investigation of the local age, and the local purging flow rate in two dimensional ventilated rooms, in: ROOMVENT-87, Stockholm, Sweden, 1987, pp. 1–14.
[19] Q. Chen, Simulation of simple cases, Swiss Federal Institute of Technology Zurich (Energy System Laboratory), Annex Report, March 1991.
[20] Q. Chen, Comparison of different k–ε models for indoor air flow computations, Numerical Heat Transfer, Part B 28 (1995) 353–369.
[21] S. Rees, J. McGuirk, P. Haves, Numerical investigations of transient buoyant flow in a room with displacement ventilation and chilled ceiling system, Int. J. Heat Mass Transfer 44 (2001) 3067–3080.
[22] J. Moureh, D. Flick, Airflow characteristics within a slot-ventilated enclosure, Int. J. Heat Fluid Flow 26 (2005) 12–24.
[23] R. Henkes, F. Van-Der-Vlugt, C. Hoogendoorn, Natural-convection flow in a square cavity calculated with low-Reynolds-number turbulence models, Int. J. Heat Mass Transfer 34 (1991) 377–388.
[24] S. Patankar, Numerical Heat Transfer and Fluid Flow, Hemisphere Publishing, Washington, 1980.
[25] J. Van Doormaal, G. Raithby, Enhancements of the SIMPLE method for predicting incompressible fluid flow, Numerical Heat Transfer 7 (1984) 147–163.
[26] ASHRAE, Handbook of Fundamentals, American Society of Heating, Refrigeration and Air Conditioning Engineers, New York, 2005.
[27] J. Tun, Análisis de la transferencia de calor conjugada en cavidades ventiladas con flujo turbulento, Master Thesis, Department of Mechanical Engineering, CENIDET, Cuernavaca Mor., Méx., 2007.